Chapter 39

Chaotic multiscattering

(A. Wirzba and P. Cvitanović)

We discuss here the semiclassics of scattering in open systems with a finite number of non-overlapping finite scattering regions. Why is this interesting at all? The semiclassics of scattering systems has five advantages compared to the bound-state problems such as the helium quantization discussed in chapter 41.

rigor, numerical accuracy, testbed for ideas

- For bound-state problem the semiclassical approximation does not respect quantum-mechanical unitarity, and the semi-classical eigenenergies are not real. Here we construct *a manifestly unitary* semiclassical scattering matrix.
- The Weyl-term contributions decouple from the multi-scattering system.
- The close relation to the classical escape processes discussed in chapter 1.

give a more precise section link

- For scattering systems the derivation of cycle expansions is more direct and controlled than in the bound-state case: the semiclassical cycle expansion is the saddle-point approximation to the cumulant expansion of the determinant of the exact quantum-mechanical multi-scattering matrix.
- The region of convergence of the semiclassical spectral function is larger than is the case for the bound-state case.

We start by a brief review of the elastic scattering of a point particle from finite collection of non-overlapping scattering regions in terms of the standard textbook scattering theory, and then develop the semiclassical scattering trace formulas and spectral determinants for scattering off N disks in a plane.

Helmholtz equation
Bessel function
Hankel function

39.1 Quantum mechanical scattering matrix

We now specialize to the elastic scattering of a point particle from finite collection of N non-overlapping reflecting disks in a 2-dimensional plane. As the point particle moves freely between the static scatterers, the time independent Schrödinger equation outside the scattering regions is the Helmholtz equation:

$$\left(\vec{\nabla}_r^2 + \vec{k}^2\right)\psi(\vec{r}) = 0\,, \qquad \vec{r}\,\text{outside the scattering regions.} \tag{39.1}$$

Here $\psi(\vec{r})$ is the wave function of the point particle at spatial position $\vec{r}$ and $E = \hbar^2\vec{k}^2/2m$ is its energy written in terms of its mass m and the wave vector $\vec{k}$ of the incident wave. For reflecting wall billiards the scattering problem is a boundary value problem with Dirichlet boundary conditions:

$$\psi(\vec{r}) = 0\,, \qquad \vec{r}\,\text{on the billiard perimeter} \tag{39.2}$$

As usual for scattering problems, we expand the wave function $\psi(\vec{r})$ in the (2-dimensional) angular momentum eigenfunctions basis

AW: changed Φ_r back to Φ_k. Note, ψ_m^k depends on $\vec{r}$.

$$\psi(\vec{r}) = \sum_{m=-\infty}^{\infty} \psi_m^k(\vec{r})e^{-im\Phi_k}\,, \tag{39.3}$$

where k and Φ_k are the length and angle of the wave vector, respectively. A plane wave in two dimensions expaned in the angular momentum basis is

AW: for consistency reasons one needs both Φ_k and Φ_r.

$$e^{i\vec{k}\cdot\vec{r}} = e^{ikr\cos(\Phi_r-\Phi_k)} = \sum_{m=-\infty}^{\infty} J_m(kr)e^{im(\Phi_r-\Phi_k)}\,, \tag{39.4}$$

where r and Φ_r denote the distance and angle of the spatial vector $\vec{r}$ as measured in the global 2-dimensional coordinate system.

The mth angular component $J_m(kr)e^{im\Phi_r}$ of a plane wave is split into a superposition of incoming and outgoing 2-dimensional spherical waves by decomposing the ordinary Bessel function $J_m(z)$ into the sum

$$J_m(z) = \frac{1}{2}\left(H_m^{(1)}(z) + H_m^{(2)}(z)\right) \tag{39.5}$$

of the Hankel functions $H_m^{(1)}(z)$ and $H_m^{(2)}(z)$ of the first and second kind. For $|z| \gg 1$ the Hankel functions behave asymptotically as:

$$\begin{aligned} H_m^{(2)}(z) &\sim \sqrt{\frac{2}{\pi z}}e^{-i(z-\frac{\pi}{2}m-\frac{\pi}{4})} \quad \text{incoming,} \\ H_m^{(1)}(z) &\sim \sqrt{\frac{2}{\pi z}}e^{+i(z-\frac{\pi}{2}m-\frac{\pi}{4})} \quad \text{outgoing.} \end{aligned} \tag{39.6}$$

Thus for $r \to \infty$ and k fixed, the mth angular component $J_m(kr)e^{im\Phi_r}$ of the plane wave can be written as superposition of incoming and outgoing 2-dimensional spherical waves:

one-disk@1-disk!scattering

$$J_m(kr)e^{im\Phi_r} \sim \frac{1}{\sqrt{2\pi kr}}\left[e^{-i(kr-\frac{\pi}{2}m-\frac{\pi}{4})} + e^{i(kr-\frac{\pi}{2}m-\frac{\pi}{4})}\right] e^{im\Phi_r} \ . \quad (39.7)$$

In terms of the asymptotic (angular momentum) components ψ_m^k of the wave function $\psi(\vec{r})$, the scattering matrix (38.3) is defined as

⇓PRELIMINARY

??
page ??

$$\psi_m^k \sim \frac{1}{\sqrt{2\pi kr}} \sum_{m'=-\infty}^{\infty} \left[\delta_{mm'} e^{-i(kr-\frac{\pi}{2}m'-\frac{\pi}{4})} + S_{mm'} e^{i(kr-\frac{\pi}{2}m'-\frac{\pi}{4})}\right] e^{im'\Phi_r} \quad (39.8)$$

⇑PRELIMINARY

The matrix element $S_{mm'}$ describes the scattering of an incoming wave with angular momentum m into an outgoing wave with angular momentum m'. If there are no scatterers, then $\mathbf{S} = \mathbf{1}$ and the asymptotic expression of the plane wave $e^{i\vec{k}\cdot\vec{r}}$ in two dimensions is recovered from $\psi(\vec{r})$.

39.1.1 1-disk scattering matrix

In general, $\mathbf{S}$ is nondiagonal and nonseparable. An exception is the 1-disk scatterer. If the origin of the coordinate system is placed at the center of the disk, by (39.5) the mth angular component of the time-independent scattering wave function is a superposition of incoming and outgoing 2-dimensional spherical waves

38.2
page 723

$$\begin{aligned} \psi_m^k &= \frac{1}{2}\left(H_m^{(2)}(kr) + S_{mm}H_m^{(1)}(kr)\right) e^{im\Phi_r} \\ &= \left(J_m(kr) - \frac{i}{2}T_{mm}H_m^{(1)}(kr)\right) e^{im\Phi_r} \ . \end{aligned}$$

The vanishing (39.2) of the wave function on the disk perimeter

$$0 = J_m(ka) - \frac{i}{2}T_{mm}H_m^{(1)}(ka)$$

yields the 1-disk scattering matrix in analytic form:

$$S^s_{mm'}(k) = \left(1 - \frac{2J_m(ka_s)}{H_m^{(1)}(ka_s)}\right)\delta_{mm'} = -\frac{H_m^{(2)}(ka_s)}{H_m^{(1)}(ka_s)}\delta_{mm'} \ , \quad (39.9)$$

where $a = a_s$ is radius of the disk and the suffix ^{s} indicates that we are dealing with a disk whose label is s. We shall derive a semiclassical approximation to this 1-disk $\mathbf{S}$-matrix in sect. 39.3.

Bessel function!addition theorem

multi-scattering matrix

39.1.2 Multi-scattering matrix

Consider next a scattering region consisting of N non-overlapping disks labeled $s \in \{1, 2, \cdots, N\}$, following the notational conventions of sect. 11.6. The strategy is to construct the full $\mathbf{T}$-matrix (38.3) from the exact 1-disk scattering matrix (39.9) by a succession of coordinate rotations and translations such that at each step the coordinate system is centered at the origin of a disk. Then the $\mathbf{T}$-matrix in $S_{mm'} = \delta_{mm'} - i\,T_{mm'}$ can be split into a product over three kinds of matrices,

Andreas, please recheck this equation

$$T_{mm'}(k) = \sum_{s,s'=1}^{N} \sum_{l_s, l_{s'}=-\infty}^{\infty} C_{ml_s}^{\ s}(k) \mathbf{M}^{-1}(k)_{l_s l_{s'}}^{s s'} D_{l_{s'} m'}^{s'}(k)\,.$$

The outgoing spherical wave scattered by the disk s is obtained by shifting the global coordinates origin distance R_s to the center of the disk s, and measuring the angle Φ_s with respect to direction $\mathbf{k}$ of the outgoing spherical wave. As in (39.9), the matrix $\mathbf{C}^s$ takes form

$$C_{ml_s}^{\ s} = \frac{2i}{\pi a_s} \frac{J_{m-l_s}(kR_s)}{H_{l_s}^{(1)}(ka_s)} e^{im\Phi_s}\,. \tag{39.10}$$

If we now describe the ingoing spherical wave in the disk s' coordinate frame by the matrix $\mathbf{D}^{s'}$

$$D_{l_{s'} m'}^{s'} = -\pi a_{s'} J_{m'-l_{s'}}(kR_{s'}) J_{l_{s'}}(ka_{s'}) e^{-im'\Phi_{s'}}\,, \tag{39.11}$$

edited to here 12jun06

looks wrong, redo!

and apply the Bessel function addition theorem

$$J_m(y+z) = \sum_{\ell=-\infty}^{\infty} J_{m-\ell}(y) J_\ell(z),$$

we recover the $\mathbf{T}$-matrix (39.9) for the single disk $s = s'$, $M = 1$ scattering. The Bessel function sum is a statement of the completness of the spherical wave basis; as we shift the origin from the disk s to the disk s' by distance $R_{s'}$, we have to reexpand all basis functions in the new coordinate frame.

The labels m and m' refer to the angular momentum quantum numbers of the ingoing and outgoing waves in the global coordinate system, and $l_s, l_{s'}$ refer to the (angular momentum) basis fixed at the sth and s'th scatterer, respectively. Thus, $\mathbf{C}^s$ and $\mathbf{D}^{s'}$ depend on the origin and orientation of the global coordinate system of the 2-dimensional plane as well as on the internal coordinates of the scatterers. As they can be made separable in the scatterer label s, they describe the single scatterer aspects of what, in general, is a multi-scattering problem.

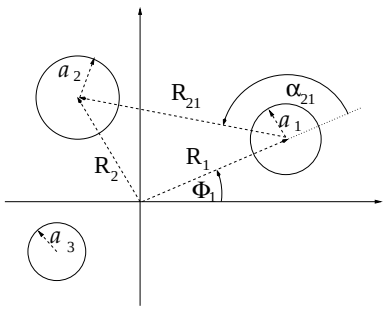

Figure 39.1: Global and local coordinates for a general 3-disk problem.

The matrix $\mathbf{M}$ is called the *multi-scattering matrix*. If the scattering problem consists only of one scatterer, $\mathbf{M}$ is simply the unit matrix $M^{ss'}_{l_s l_{s'}} = \delta^{ss'}\delta_{l_s l_{s'}}$. For scattering from more than one scatterer we separate out a "single traversal" matrix $\mathbf{A}$ which transports the scattered wave from a scattering region $\mathcal{M}_s$ to the scattering region $\mathcal{M}_{s'}$,

a multiscattered ctory illustrating expansion of $\mathbf{M}^{-1}$

Note that talk here about tum mechanics. rajectory is not ningful, yet. If wants to draw ething, it should avefront.

Changed the sign of $\mathbf{A}$ throughout, in deference to DasBuch notational conventions

$$M^{ss'}_{l_s l_{s'}} = \delta^{ss'}\delta_{l_s l_{s'}} - A^{ss'}_{l_s l_{s'}} \,. \tag{39.12}$$

The matrix $\mathbf{A}^{ss'}$ reads:

$$A^{ss'}_{l_s l_{s'}} = -(1-\delta^{ss'})\,\frac{a_s}{a_{s'}}\,\frac{J_{l_s}(ka_s)}{H^{(1)}_{l_{s'}}(ka_{s'})}\,H^{(1)}_{l_s - l_{s'}}(kR_{ss'})\,e^{i(l_s\alpha_{s's}-l_{s'}(\alpha_{ss'}-\pi))}\,. \tag{39.13}$$

Here, a_s is the radius of the sth disk. R_s and Φ_s are the distance and angle, respectively, of the ray from the origin in the 2-dimensional plane to the center of disk s as measured in the global coordinate system. Furthermore, $R_{ss'} = R_{s's}$ is the separation between the centers of the sth and s'th disk and $\alpha_{s's}$ of the ray from the center of disk s to the center of disk s' as measured in the local (body-fixed) coordinate system of disk s (see figure 39.1).

Expanded as a geometrical series about the unit matrix $\mathbf{1}$, the inverse matrix $\mathbf{M}^{-1}$ generates a multi-scattering series in powers of the single-traversal matrix $\mathbf{A}$. All genuine multi-scattering dynamics is contained in the matrix $\mathbf{A}$; by construction $\mathbf{A}$ vanishes for a single-scatterer system.

39.2 N-scatterer spectral determinant

In the following we limit ourselves to a study of the spectral properties of the $\mathbf{S}$-matrix: resonances, time delays and phase shifts. The resonances are given by the poles of the $\mathbf{S}$-matrix in the lower complex wave number (k) plane; more precisely, by the poles of the $\mathbf{S}$ on the second Riemann sheet of the complex energy plane. As the $\mathbf{S}$-matrix is unitary, it is also natural to focus on its total phase shift $\eta(k)$ defined by $\det \mathbf{S} = \exp^{2i\eta(k)}$. The

δ_m? see (38.5)

trace!-class operators

time-delay is proportional to the derivative of the phase shift with respect to the wave number k.

As we are only interested in spectral properties of the scattering problem, it suffices to study $\det \mathbf{S}$. This determinant is basis and coordinate-system independent, whereas the $\mathbf{S}$-matrix itself depends on the global coordinate system and on the choice of basis for the point particle wave function.

As the $\mathbf{S}$-matrix is, in general, an infinite dimensional matrix, it is not clear whether the corresponding determinant exists at all. If $\mathbf{T}$-matrix is trace-class, the determinant does exist. What does this mean?

39.2.1 Trace-class operators

An operator (an infinite-dimensional matrix) is called *trace-class* if and only if, for any choice of orthonormal basis, the sum of the diagonal matrix elements converges absolutely; it is called "Hilbert-Schmidt", if the sum of the absolute squared diagonal matrix elements converges. Once an operator is diagnosed as trace-class, we are allowed to manipulate it as we manipulate finite-dimensional matrices. We review the theory of trace-class operators in appendix M; here we will assume that the $\mathbf{T}$-matrix (38.3) is trace-class, and draw the conlusions.

If $\mathbf{A}$ is trace-class, the determinant $\det(\mathbf{1} - z\mathbf{A})$, as defined by the cumulant expansion, exists and is an entire function of z. Furthermore, the determinant is invariant under any unitary transformation.

add links to earlier materail, exercises

The cumulant expansion is the analytical continuation (as Taylor expansion in the book-keeping variable z) of the determinant

$$\det(\mathbf{1} - z\mathbf{A}) = \exp[\mathrm{tr}\,\ln(\mathbf{1} - z\mathbf{A})] = \exp\left(-\sum_{n=1}^{\infty}\frac{z^n}{z^n}\mathrm{tr}\,(\mathbf{A}^n)\right)\ .$$

That means

$$\det(\mathbf{1} - z\mathbf{A}) := \sum_{m=0}^{\infty} z^m Q_m(\mathbf{A})\ , \tag{39.14}$$

where the cumulants $Q_m(\mathbf{A})$ satisfy the Plemelj-Smithies recursion formula (M.26), a generalization of Newton's formula to determinants of infinite-dimensional matrices,

fix reference to (M.26) or d-cyc-exp?

$$\begin{aligned} Q_0(\mathbf{A}) &= 1 \\ Q_m(\mathbf{A}) &= -\frac{1}{m}\sum_{j=1}^{m} Q_{m-j}(\mathbf{A})\,\mathrm{tr}\,(\mathbf{A}^j) \quad \text{for } m \geq 1\,, \end{aligned} \tag{39.15}$$

in terms of cumulants of order $n < m$ and traces of order $n \leq m$. Because of the trace-class property of $\mathbf{A}$, all cumulants and traces exist separately.

For the general case of $N < \infty$ non-overlapping scatterers, the $\mathbf{T}$-matrix can be shown to be trace-class, so the determinant of the $\mathbf{S}$-matrix is well defined. What does trace-class property mean for the corresponding matrices $\mathbf{C}^s$, $\mathbf{D}^s$ and $\mathbf{A}^{ss'}$? Manipulating the operators as though they were finite matrices, we can perform the following transformations:

$$\begin{aligned} \det \mathbf{S} &= \det \left(\mathbf{1} - i\mathbf{C}\mathbf{M}^{-1}\mathbf{D}\right) \\ &= \mathrm{Det}\, \left(\mathbf{1} - i\mathbf{M}^{-1}\mathbf{D}\mathbf{C}\right) \,=\, \mathrm{Det}\, \left(\mathbf{M}^{-1}(\mathbf{M} - i\mathbf{D}\mathbf{C})\right) \\ &= \frac{\mathrm{Det}\,(\mathbf{M} - i\mathbf{D}\mathbf{C})}{\mathrm{Det}\,(\mathbf{M})} \,. \,. \end{aligned} \tag{39.16}$$

In the first line of (39.16) the determinant is taken over small ℓ (the angular momentum with respect to the global system). In the remainder of (39.16) the determinant is evaluated over the multiple indices $L_s = (s, l_s)$. In order to signal this difference we use the following notation: det ... and tr ... refer to the $|\ell\rangle$ space, Det ... and Tr ... refer to the multiple index space. The matrices in the multiple index space are expanded in the complete basis $\{|L_s\rangle\} = \{|s, \ell_s\rangle\}$ which refers for fixed index s to the origin of the sth scatterer and not any longer to the origin of the 2-dimensional plane.

Let us explicitly extract the product of the determinants of the subsystems from the determinant of the total system (39.16):

$$\begin{aligned} \det \mathbf{S} &= \frac{\mathrm{Det}\,(\mathbf{M} - i\mathbf{D}\mathbf{C})}{\mathrm{Det}\,(\mathbf{M})} \\ &= \frac{\mathrm{Det}\,(\mathbf{M} - i\mathbf{D}\mathbf{C})}{\mathrm{Det}\,\mathbf{M}} \frac{\prod_{s=1}^{N} \det \mathbf{S}^s}{\prod_{s=1}^{N} \det \mathbf{S}^s} \\ &= \left(\prod_{s=1}^{N} \det \mathbf{S}^s\right) \frac{\mathrm{Det}\,(\mathbf{M} - i\mathbf{D}\mathbf{C}) / \prod_{s=1}^{N} \det \mathbf{S}^s}{\mathrm{Det}\,\mathbf{M}} \,. \end{aligned} \tag{39.17}$$

The final step in the reformulation of the determinant of the $\mathbf{S}$-matrix of the N-scatterer problem follows from the unitarity of the $\mathbf{S}$-matrix. The unitarity of $\mathbf{S}^\dagger(k^*)$ implies for the determinant find refeq S-unitary

$$\det\left(\mathbf{S}(k^*)^\dagger\right) = 1/\det \mathbf{S}(k)\,, \tag{39.18}$$

where this manipulation is allowed because the $\mathbf{T}$-matrix is trace-class. The unitarity condition should apply for the $\mathbf{S}$-matrix of the total system, $\mathbf{S}$, as for the each of the single subsystems, $\mathbf{S}^s$, $s = 1, \cdots, N$. In terms of the result of (39.17), this implies

$$\frac{\mathrm{Det}\,(\mathbf{M}(k) - i\mathbf{D}(k)\mathbf{C}(k))}{\prod_{s=1}^{N} \det \mathbf{S}^s} = \mathrm{Det}\,(\mathbf{M}(k^*)^\dagger)$$

since all determinants in (39.17) exist separately and since the determinants $\det \mathbf{S}^s$ respect unitarity by themselves. Thus, we finally have

$$\det \mathbf{S}(k) = \left\{ \prod_{s=1}^{N} (\det \mathbf{S}^s(k)) \right\} \frac{\mathrm{Det}\, \mathbf{M}(k^*)^\dagger}{\mathrm{Det}\, \mathbf{M}(k)} \,, \tag{39.19}$$

where all determinants exist separately.

In summary: We assumed a scattering system of a *finite* number of *non-overlapping* scatterers which can be of different shape and size, but are all of finite extent. We assumed the trace-class character of the **T**-matrix belonging to the total system and of the single-traversal matrix **A** and finally unitarity of the **S**-matrices of the complete and all subsystems.

What can one say about the point-particle scattering from a finite number of scatterers of arbitrary shape and size? As long as each of $N < \infty$ single scatterers has a finite spatial extent, i.e., can be covered by a finite disk, the total system has a finite spatial extent as well. Therefore, it too can be put insided a circular domain of finite radius b, e.g., inside a single disk. If the impact parameter of the point particle measured with respect to the origin of this disk is larger than the disk size (actually larger than $(e/2) \times b$), then the **T** matrix elements of the N-scatterer problem become very small. If the wave number k is kept fixed, the modulus of the *diagonal* matrix elements, $|T_{mm}|$ with the angular momentum $m > (e/2)kb$, is bounded by the corresponding quantity of the covering disk.

39.2.2 Quantum cycle expansions

In formula (39.19) the genuine multi-scattering terms are separated from the single-scattering ones. We focus on the multi-scattering terms, i.e., on the ratio of the determinants of the multi-scattering matrix $\mathbf{M} = \mathbf{1} - \mathbf{A}$ in (39.19), since they are the origin of the periodic orbit sums in the semiclassical reduction. The resonances of the multi-scattering system are given by the zeros of $\mathrm{Det}\, \mathbf{M}(k)$ in the lower complex wave number plane.

In order to set up the problem for the semiclassical reduction, we express the determinant of the multi-scattering matrix in terms of the traces of the powers of the matrix **A**, by means of the cumulant expansion (39.14). Because of the finite number $N \geq 2$ of scatterers $\mathrm{tr}\,(\mathbf{A}^n)$ receives contributions corresponding to all periodic itineraries $s_1 s_2 s_3 \cdots s_{n-1} s_n$ of total symbol length n with an alphabet $s_i \in \{1, 2, \ldots, N\}$. of N symbols,

$$\begin{aligned} &\mathrm{tr}\, \mathbf{A}^{s_1 s_2} \mathbf{A}^{s_2 s_3} \cdots \mathbf{A}^{s_{n-1} s_n} \mathbf{A}^{s_n s_n} \\ &= \sum_{l_{s_1}=-\infty}^{+\infty} \sum_{l_{s_2}=-\infty}^{+\infty} \cdots \sum_{l_{s_n}=-\infty}^{+\infty} A^{s_1 s_2}_{l_{s_1} l_{s_2}} A^{s_2 s_3}_{l_{s_2} l_{s_3}} \cdots A^{s_{n-1} s_n}_{l_{s_{n-1}} l_{s_n}} A^{s_n s_1}_{l_{s_n} l_{s_1}} \,. \end{aligned} \tag{39.20}$$

Remember our notation that the trace $\mathrm{tr}\,(\cdots)$ refers only to the $|l\rangle$ space. By construction $\mathbf{A}$ describes only scatterer-to-scatterer transitions, so the symbolic dynamics has to respect the no-self-reflection pruning rule: for admissible itineraries the successive symbols have to be different. This rule is implemented by the factor $1-\delta^{ss'}$ in (39.13).

one-disk@1-disk!semiclassical scattering

The trace $\mathrm{tr}\,\mathbf{A}^n$ is the sum of all itineraries of length n,

$$\mathrm{tr}\,\mathbf{A}^n = \sum_{\{s_1 s_2 \cdots s_n\}} \mathrm{tr}\,\mathbf{A}^{s_1 s_2}\mathbf{A}^{s_2 s_3}\cdots\mathbf{A}^{s_{n-1}s_n}\mathbf{A}^{s_n s_1}\ . \tag{39.21}$$

We will show for the N-disk problem that these periodic itineraries correspond in the semiclassical limit, $ka_{s_i} \gg 1$, to *geometrical* periodic orbits with the same symbolic dynamics.

move this to a better place

For periodic orbits with creeping sections the symbolic alphabet has to be extended, see sect. 39.3.1. Furthermore, depending on the geometry, there might be nontrivial pruning rules based on the so called ghost orbits, see sect. 39.4.1.

39.2.3 Symmetry reductions

change to Det $\mathbf{M}$ in def.tex

The determinants over the multi-scattering matrices run over the multiple index L of the multiple index space. This is the proper form for the symmetry reduction (in the multiple index space), e.g., if the scatterer configuration is characterized by a discrete symmetry group G, we have

$$\mathrm{Det}\,\mathbf{M} = \prod_{\alpha} \left(\det \mathbf{M}_{\mathrm{D}_\alpha}(k)\right)^{d_\alpha}\ ,$$

where the index α runs over all conjugate classes of the symmetry group G and D_α is the αth representation of dimension d_α. The symmetry reduction on the exact quantum mechanical level is the same as for the classical evolution operators spectral determinant factorization (22.17) of sect. 22.4.2.

39.3 Semiclassical 1-disk scattering

We start by focusing on the single-scatterer problem. In order to be concrete, we will consider the semiclassical reduction of the scattering of a single disk in plane.

Instead of calculating the semiclassical approximation to the determinant of the one-disk system scattering matrix (39.9), we do so for

why boldface $\mathbf{d}(k)$?

$$\mathbf{d}(k) \equiv \frac{1}{2\pi i}\frac{d}{dk}\ln\det \mathbf{S}^1(ka) \ = \frac{1}{2\pi i}\frac{d}{dk}\mathrm{tr}\,\left(\ln \mathbf{S}^1(ka)\right) \tag{39.22}$$

might want to connect this to (18.21), the expection value of time

the so called *time delay*.

$$\begin{aligned}\mathbf{d}(k) &= \frac{1}{2\pi i}\frac{d}{dk}\mathrm{tr}\,\left(\ln\det \mathbf{S}^1(ka)\right) = \frac{1}{2\pi i}\sum_m \left(\frac{H_m^{(1)}(ka)}{H_m^{(2)}(ka)}\,\frac{d}{dk}\frac{H_m^{(2)}(ka)}{H_m^{(1)}(ka)}\right)\\ &= \frac{a}{2\pi i}\sum_m\left(\frac{H_m^{(2)\prime}(ka)}{H_m^{(2)}(ka)} - \frac{H_m^{(1)\prime}(ka)}{H_m^{(1)}(ka)}\right)\ .\end{aligned} \tag{39.23}$$

Here the prime denotes the derivative with respect to the argument of the Hankel functions. Let us introduce the abbreviation

$$\chi_\nu = \frac{H_\nu^{(2)\prime}(ka)}{H_\nu^{(2)}(ka)} - \frac{H_\nu^{(1)\prime}(ka)}{H_\nu^{(1)}(ka)}\ . \tag{39.24}$$

We apply the Watson contour method to (39.23)

$$\mathbf{d}(k) = \frac{a_j}{2\pi i}\sum_{m=-\infty}^{+\infty}\chi_m = \frac{a_j}{2\pi i}\,\frac{1}{2i}\oint_C \mathrm{d}\nu\,\frac{e^{-i\nu\pi}}{\sin(\nu\pi)}\chi_\nu\ . \tag{39.25}$$

Here the contour C encircles in a counter-clockwise manner a small semiinfinite strip D which completely covers the real ν-axis but which only has a small finite extent into the positive and negative imaginary ν direction. The contour C is then split up in the path above and below the real ν-axis such that

$$\mathbf{d}(k) = \frac{a}{4\pi i}\left\{\int_{-\infty+i\epsilon}^{+\infty+i\epsilon}\mathrm{d}\nu\,\frac{e^{-i\nu\pi}}{\sin(\nu\pi)}\chi_\nu - \int_{-\infty-i\epsilon}^{+\infty-i\epsilon}\mathrm{d}\nu\,\frac{e^{-i\nu\pi}}{\sin(\nu\pi)}\chi_\nu\right\}\ .$$

Then, we perform the substitution $\nu\to-\nu$ in the second integral so as to get

$$\begin{aligned}\mathbf{d}(k) &= \frac{a}{4\pi}\left\{\int_{-\infty+i\epsilon}^{+\infty+i\epsilon}\mathrm{d}\nu\,\frac{e^{-i\nu\pi}}{\sin(\nu\pi)}\chi_\nu + \mathrm{d}\nu\,\frac{e^{+i\nu\pi}}{\sin(\nu\pi)}\chi_{-\nu}\right\}\\ &= \frac{a}{2\pi i}\left\{2\int_{-\infty+i\epsilon}^{+\infty+i\epsilon}\mathrm{d}\nu\,\frac{e^{2i\nu\pi}}{1-e^{2i\nu\pi}}\,\chi_\nu + \int_{-\infty}^{+\infty}\mathrm{d}\nu\,\chi_\nu\right\}\ ,\end{aligned} \tag{39.26}$$

where we used the fact that $\chi_{-\nu}=\chi_\nu$. The contour in the last integral can be deformed to pass over the real ν-axis since its integrand has no Watson denominator.

Airy function
Airy function

We will now approximate the last expression semiclassically, i.e., under the assumption $ka \gg 1$. As the two contributions in the last line of (39.26) differ by the presence or absence of the Watson denominator, they will have to be handled semiclassically in different ways: the first will be closed in the upper complex plane and evaluated at the poles of χ_ν, the second integral will be evaluated on the real ν-axis under the Debye approximation for Hankel functions.

We will now work out the first term. The poles of χ_ν in the upper complex plane are given by the zeros of $H_\nu^{(1)}(ka)$ which will be denoted by $\nu_\ell(ka)$ and by the zeros of $H_\nu^{(2)}(ka)$ which we will denote by $-\bar\nu_\ell(ka)$, $\ell = 1, 2, 3, \cdots$. In the Airy approximation to the Hankel functions they are given by

$$\begin{aligned} \nu_\ell(ka) &= ka + i\alpha_\ell(ka)\ , && (39.27)\\ -\bar\nu_\ell(ka) &= -ka + i(\alpha_\ell(k^*a))^* = -\left(\nu_\ell(k^*a)\right)^*\ , && (39.28) \end{aligned}$$

with

refer to occurances of Airy fcts in simpler settings, such as in the $1-d$ WKB

$$\begin{aligned} i\alpha_\ell(ka) &= e^{i\frac{\pi}{3}}\left(\frac{ka}{6}\right)^{1/3} q_\ell \;-\; e^{-i\frac{\pi}{3}}\left(\frac{6}{ka}\right)^{1/3}\frac{q_\ell^2}{180} \;-\; \frac{1}{70ka}\left(1-\frac{q_\ell^3}{30}\right)\\ &+ e^{i\frac{\pi}{3}}\left(\frac{6}{ka}\right)^{\frac{5}{3}}\frac{1}{3150}\left(\frac{29q_\ell}{6^2}-\frac{281q_\ell^4}{180\cdot 6^3}\right) + \cdots . \qquad (39.29) \end{aligned}$$

Here q_ℓ labels the zeros of the Airy integral

$$A(q) \equiv \int_0^\infty \mathrm{d}\tau\ \cos(q\tau - \tau^3) = 3^{-1/3}\pi \mathrm{Ai}(-3^{-1/3}q)\ ,$$

with $\mathrm{Ai}(z)$ being the standard Airy function; approximately, $q_\ell \approx 6^{1/3}[3\pi(\ell - 1/4)]^{2/3}/2$. In order to keep the notation simple, we will abbreviate $\nu_\ell \equiv \nu_\ell(ka)$ and $\bar\nu_\ell \equiv \bar\nu_\ell(ka)$. Thus the first term of (39.26) becomes finally

$$\frac{a}{2\pi i}\left\{2\int_{-\infty+i\epsilon}^{+\infty+i\epsilon}\mathrm{d}\nu\ \frac{e^{2i\nu\pi}}{1-e^{2i\nu\pi}}\,\chi_\nu\right\} = 2a\sum_{\ell=1}^{\infty}\left(\frac{e^{2i\nu_\ell\pi}}{1-e^{2i\nu_\ell\pi}} + \frac{e^{-2i\bar\nu_\ell\pi}}{1-e^{-2i\bar\nu_\ell\pi}}\right).$$

In the second term of (39.26) we will insert the Debye approximations for the Hankel functions:

$$\begin{aligned} H_\nu^{(1/2)}(x) &\sim \sqrt{\frac{2}{\pi\sqrt{x^2-\nu^2}}}\exp\left(\pm i\sqrt{x^2-\nu^2} \mp i\nu\arccos\frac{\nu}{x} \mp i\frac{\pi}{4}\right) \quad \text{for } |x| > \nu \qquad (39.30)\\ H_\nu^{(1/2)}(x) &\sim \mp i\sqrt{\frac{2}{\pi\sqrt{\nu^2-x^2}}}\exp\left(-\sqrt{\nu^2-x^2} + \nu\,\mathrm{ArcCosh}\frac{\nu}{x}\right) \qquad \text{for } |x| < \nu\ . \end{aligned}$$

one-disk@1-disk!creeping
creeping!1-disk

Note that for $\nu > ka$ the contributions in χ_ν cancel. Thus the second integral of (39.26) becomes

$$\begin{aligned}\frac{a}{2\pi i}\int_{-\infty}^{+\infty} \mathrm{d}\nu\, \chi_\nu &= \frac{a}{2\pi i}\int_{-ka}^{+ka} \mathrm{d}\nu\, \frac{(-2i)}{a}\frac{d}{dk}\left(\sqrt{k^2a^2-\nu^2} - \nu \arccos\frac{\nu}{ka}\right) + \cdots \\ &= -\frac{1}{k\pi}\int_{-ka}^{ka} \mathrm{d}\nu \sqrt{k^2a^2-\nu^2} + \cdots = -\frac{a^2}{2}k + \cdots\ , \qquad (39.31)\end{aligned}$$

where $\cdots$ takes care of the polynomial corrections in the Debye approximation and the boundary correction terms in the ν integration.

In summary, the semiclassical approximation to $\mathbf{d}(k)$ reads

$$\mathbf{d}(k) = 2a\sum_{\ell=1}^{\infty}\left(\frac{e^{2i\nu_\ell\pi}}{1-e^{2i\nu_\ell\pi}} + \frac{e^{-2i\bar{\nu}_\ell\pi}}{1-e^{-2i\bar{\nu}_\ell\pi}}\right) - \frac{a^2}{2}k + \cdots\ .$$

Using the definition of the time delay (39.22), we get the following expression for $\det \mathbf{S}^1(ka)$:

$$\begin{aligned}&\ln\det\mathbf{S}^1(ka) - \lim_{k_0\to 0}\ln\det\mathbf{S}^1(k_0a) \qquad (39.32)\\ &= 2\pi i a\int_0^k \mathrm{d}\tilde{k}\left(-\frac{a\tilde{k}}{2} + 2\sum_{\ell=1}^{\infty}\left(\frac{e^{i2\pi\nu_\ell(\tilde{k}a)}}{1-e^{i2\pi\nu_\ell(\tilde{k}a)}} + \frac{e^{-i2\pi\bar{\nu}_\ell(\tilde{k}a)}}{1-e^{-i2\pi\bar{\nu}_\ell(\tilde{k}a)}}\right)\right) + \cdots \\ &\sim -2\pi i N(k) + 2\sum_{\ell=1}^{\infty}\int_0^k \mathrm{d}\tilde{k}\,\frac{d}{d\tilde{k}}\left\{-\ln\left(1-e^{i2\pi\nu_\ell(\tilde{k}a)}\right) + \ln\left(1-e^{-i2\pi\bar{\nu}_\ell(\tilde{k}a)}\right)\right\} + \cdots,\end{aligned}$$

where in the last expression it has been used that semiclassically $\frac{d}{dk}\nu_\ell(ka) \sim \frac{d}{dk}\bar{\nu}_\ell(ka) \sim a$ and that the Weyl term for a single disk of radius a goes like $N(k) = \pi a^2k^2/(4\pi) + \cdots$ (the next terms come from the boundary terms in the ν-integration in (39.31)). Note that for the lower limit, $k_0 \to 0$, we have two simplifications: First,

$$\begin{aligned}\lim_{k_0\to 0} S^1_{mm'}(k_0a) = \lim_{k_0\to 0}\frac{-H^{(2)}_m(k_0a)}{H^{(1)}_m(k_0a)}\delta_{mm'} &= 1\times\delta_{mm'} \qquad \forall m,m' \\ \to \lim_{k_0\to 0}\det\mathbf{S}^1(k_0a) &= 1\ .\end{aligned}$$

Secondly, for $k_0 \to 0$, the two terms in the curly bracket of (39.32) cancel.

39.3.1 1-disk spectrum interpreted; pure creeping

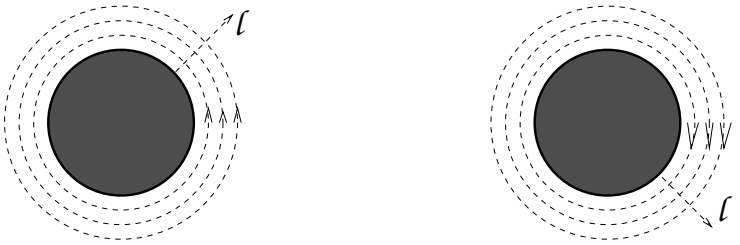

Figure 39.2: Right- and left-handed diffractive creeping paths of increasing mode number ℓ for a single disk.

To summarize: the semiclassical approximation to the determinant $\mathbf{S}^1(ka)$ is given by

$$\det \mathbf{S}^1(ka) \sim e^{-i2\pi N(k)} \frac{\prod_{\ell=1}^{\infty} \left(1 - e^{-2i\pi\bar{\nu}_\ell(ka)}\right)^2}{\prod_{\ell=1}^{\infty} \left(1 - e^{2i\pi\nu_\ell(ka)}\right)^2} , \tag{39.33}$$

with

$$\begin{array}{rclcl} \nu_\ell(ka) & = & ka + i\alpha_\ell(ka) & = & ka + e^{+i\pi/3}(ka/6)^{1/3} q_\ell + \cdots \\ \bar{\nu}_\ell(ka) & = & ka - i(\alpha_\ell(k^*a))^* & = & ka + e^{-i\pi/3}(ka/6)^{1/3} q_\ell + \cdots \\ & = & (\nu_\ell(k^*a))^* & & \end{array}$$

and $N(ka) = (\pi a^2 k^2)/4\pi + \cdots$ the leading term in the Weyl approximation for the staircase function of the wavenumber eigenvalues in the disk interior. From the point of view of the scattering particle, the interior domains of the disks are excluded relatively to the free evolution without scattering obstacles. Therefore the negative sign in front of the Weyl term. For the same reason, the subleading boundary term has here a Neumann structure, although the disks have Dirichlet boundary conditions.

Let us abbreviate the r.h.s. of (39.33) for a disk s as

$$\det \mathbf{S}^s(ka_s) \sim \left(e^{-i\pi N(ka_s)}\right)^2 \frac{\widetilde{Z}^s_\ell(k^*a_s)^*}{\widetilde{Z}^s_\ell(ka_s)} \frac{\widetilde{Z}^s_r(k^*a_s)^*}{\widetilde{Z}^s_r(ka_s)} , \tag{39.34}$$

where $\widetilde{Z}^s_\ell(ka_s)$ and $\widetilde{Z}^s_r(ka_s)$ are the *diffractional* zeta functions (here and in the following we will label semiclassical zeta functions *with* diffractive corrections by a tilde) for creeping orbits around the sth disk in the left-handed sense and the right-handed sense, respectively (see figure 39.2). The two orientations of the creeping orbits are the reason for the exponents 2 in (39.33). Equation (39.33) describes the semiclassical approximation to the incoherent part (= the curly bracket on the r.h.s.) of the exact expression (39.19) for the case that the scatterers are disks.

In the following we will discuss the semiclassical resonances in the 1-disk scattering problem with Dirichlet boundary conditions, i.e. the so-called

Airy function

shape resonances. The quantum mechanical resonances are the poles of the S-matrix in the complex k-plane. As the 1-disk scattering problem is separable, the S-matrix is already diagonalized in the angular momentum eigenbasis and takes the simple form (39.9). The exact quantummechanical poles of the scattering matrix are therefore given by the the zeros, $k^{\rm res}_{n\,m}$, of the Hankel functions $H^{(1)}_m(ka)$ in the lower complex k plane which can be labeled by two indices, m and n, where m denotes the angular quantum number of the Hankel function and n is a radial quantum number. As the Hankel functions have to vanish at specific k values, one cannot use the usual Debye approximation as semiclassical approximation for the Hankel function, since this approximation only works in case the Hankel function is dominated by only one saddle. However, for the vanishing of the Hankel function, one has to have the interplay of two saddles, thus an Airy approximation is needed as in the case of the creeping poles discussed above. The Airy approximation of the Hankel function $H^{(1)}_\nu(ka)$ of complex-valued index ν reads

$$H^{(1)}_\nu(ka) \sim \frac{2}{\pi} e^{-i\frac{\pi}{3}} \left(\frac{6}{ka}\right)^{1/3} A(q^{(1)}) \,,$$

with

$$q^{(1)} = e^{-i\frac{\pi}{3}} \left(\frac{6}{ka}\right)^{1/3} (\nu - ka) + \mathcal{O}\left((ka)^{-1}\right).$$

Hence the zeros ν_ℓ of the Hankel function in the complex ν plane follow from the zeros q_ℓ of the Airy integral $A(q)$ (see (39.3). Thus if we set $\nu_\ell = m$ (with m integer), we have the following semiclassical condition on $k^{\rm res}$

repeat of (39.29)?

$$\begin{aligned} m &\sim k^{\rm res}a + i\alpha_\ell(k^{\rm res}a) \\ &= e^{i\frac{\pi}{3}} \left(\frac{k^{\rm res}a}{6}\right)^{1/3} q_\ell \;-\; e^{-i\frac{\pi}{3}} \left(\frac{6}{k^{\rm res}a}\right)^{1/3} \frac{q_\ell^2}{180} \;-\; \frac{1}{70k^{\rm res}a} \Big(\\ &+ e^{i\frac{\pi}{3}} \left(\frac{6}{k^{\rm res}a}\right)^{\frac{5}{3}} \frac{1}{3150} \left(\frac{29q_\ell}{6^2} - \frac{281q_\ell^4}{180\cdot 6^3}\right) + \cdots, \end{aligned}$$

with $l = 1, 2, 3, \cdots$.

For a given index l this is equivalent to

$$0 \sim 1 - e^{(ik^{\rm res} - \alpha_\ell)2\pi a} \,,$$

the de-Broglie condition on the wave function that encircles the disk. Thus the semiclassical resonances of the 1-disk problem are given by the zeros of the following product

$$\prod_{l=1}^{\infty} \left(1 - e^{(ik - \alpha_\ell)2\pi a}\right),$$

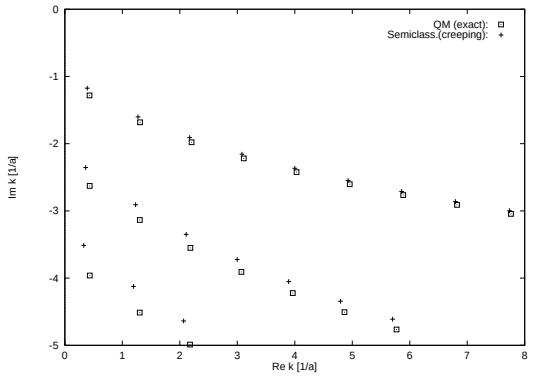

Figure 39.3: The shape resonances of the 1-disk system in the complex k plane in units of the disk radius a. The boxes label the exact quantum mechanical resonances (given by the zeros of $H_m^{(1)}(ka)$ for $m = 0, 1, 2$), the crosses label the diffractional semiclassical resonances (given by the zeros of the creeping formula in the Airy approximation (39.35) up to the order $\mathcal{O}([ka]^{1/3})$).

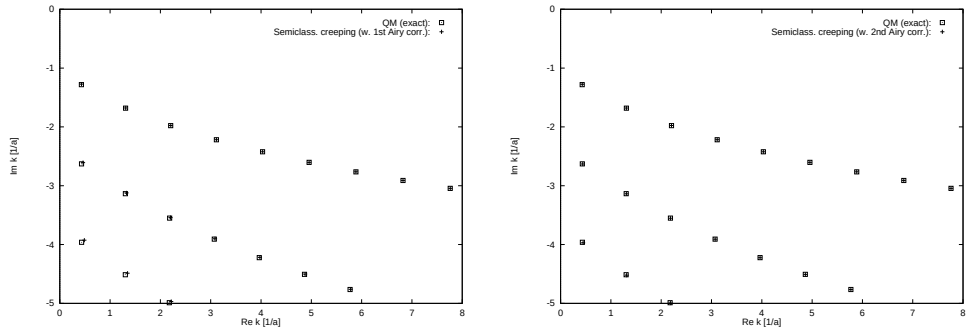

Figure 39.4: Same as in figure 39.3. However, the subleading terms in the Airy approximation (39.35) are taken into account up to the order $\mathcal{O}([ka]^{-1/3})$ (upper panel) and up to order $\mathcal{O}([ka]^{-1})$ (lower panel).

which is of course nothing else than $\widetilde{Z}_{\text{1-disk}}(k)$, the semiclassical diffraction zeta function of the 1-disk scattering problem, see (39.34). Note that this expression includes just the pure creeping contribution and no genuine geometrical parts. Because of

$$H_{-m}^{(1)}(ka) = (-1)^m H_m^{(1)}(ka)\,,$$

the zeros are doubly degenerate if $m \neq 0$, corresponding to right- and left handed creeping turns. The case $m = 0$ is unphysical, since all zeros of the Hankel function $H_0^{(1)}(ka)$ have negative real value.

From figure 39.3 one notes that the creeping terms in the Airy order $\mathcal{O}([ka]^{1/3})$, which are used in the Keller construction, systematically underestimate the magnitude of the imaginary parts of the exact data. However, the creeping data become better for increasing $\mathrm{Re}\, k$ and decreasing $|\mathrm{Im}\, k|$, as they should as semiclassical approximations.

explain Keller principle somewhere

In the upper panel of figure 39.4 one sees the change, when the next order in the Airy approximation (39.35) is taken into account. The approximation

is nearly perfect, especially for the leading row of resonances. The second Airy approximation using (39.35) up to order $\mathcal{O}([ka]^{-1})$ is perfect up to the drawing scale of figure 39.4 (lower panel).

⇓PRELIMINARY

We shall return to creeping contributions for $N > 1$ disk systems in chapter 42.

⇑PRELIMINARY

39.4 From quantum cycle to semiclassical cycle

The procedure for the semiclassical approximation of a general periodic itinerary (39.20) of length n is somewhat laborious, and we will only sketch the procedure here. It follows, in fact, rather closely the methods developed for the semiclassical reduction of the determinant of the 1-disk system.

The quantum cycle

$$\operatorname{tr} \mathbf{A}^{s_1 s_2} \cdots \mathbf{A}^{s_m s_1} = \sum_{l_{s_1}=-\infty}^{\infty} \cdots \sum_{l_{s_m}=-\infty}^{\infty} A^{s_1 s_2}_{l_{s_1} l_{s_2}} \cdots A^{s_m s_1}_{l_{s_m} l_{s_1}}$$

still has the structure of a "multi-trace" with respect to angular momentum.

Each of the sums $\sum_{l_{s_i}=-\infty}^{\infty}$ – as in the 1-disk case – is replaced by a *Watson contour* resummation in terms of complex angular momentum ν_{s_i}. Then the paths below the real ν_{s_i}-axes are transformed to paths above these axes, and the integrals split into expressions *with* and *without* an explicit Watson $\sin(\nu_{s_i}\pi)$ denominator.

1. In the $\sin(\nu_{s_i}\pi)$ -independent integrals we replace all Hankel and Bessel functions by Debye approximations. Then we evaluate the expression in the saddle point approximation: either left or right *specular reflection* at disk s_i or *ghost tunneling* through disk s_i result.

2. For the $\sin(\nu_{s_i}\pi)$ -dependent integrals, we close the contour in the upper ν_{s_i} plane and evaluate the integral at the residua $H^{(1)}_{\nu_{s_i}}(ka_{s_i})$=0. Then we use the Airy approximation for $J_{\nu_{s_i}}(ka_{s_i})$ and $H^{(1)}_{\nu_{s_i}}(ka_{s_i})$: left and right *creeping paths* around disk s_i result.

In the above we have assumed that no grazing geometrical paths appear. If they do show up, the analysis has to be extended to the case of coninciding saddles between the geometrical paths with $\pi/2$ angle reflection from the disk surface and paths with direct ghost tunneling through the disk.

There are three possibilities of "semiclassical" contact of the point particle with the disk s_i:

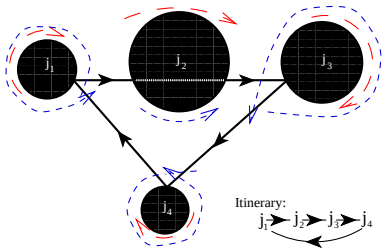

Figure 39.5: A 4-disk problem with three specular reflections, one ghost tunneling, and distinct creeping segments from which all associated creeping paths can be constructed.

1. either geometrical which in turn splits into three alternatives
   (a) *specular reflection* to the right,
   (b) *specular reflection* to the left,
   (c) or *'ghost tunneling'* where the latter induce the nontrivial pruning rules (as discussed above)
2. or *right-handed creeping turns*
3. or *left-handed creeping turns*,

see figure 39.5. The specular reflection to the right is linked to left-handed creeping paths with at least one knot. The specular reflection to the left matches a right-handed creeping paths with at least one knot, whereas the shortest left- and right-handed creeping paths in the ghost tunneling case are topologically trivial. In fact, the topology of the creeping paths encodes the choice between the three alternatives for the geometrical contact with the disk. This is the case for the simple reason that creeping sections have to be positive definite in length: the creeping amplitude has to decrease during the creeping process, as tangential rays are constantly emitted. In mathematical terms, it means that the creeping angle has to be positive. Thus, the positivity of the *two* creeping angles for the shortest left *and* right turn uniquely specifies the topology of the creeping sections which in turn specifies which of the three alternatives, either specular reflection to the right or to the left or straight "ghost" tunneling through disk j, is realized for the semiclassical geometrical path. Hence, the existence of a unique saddlepoint is guaranteed.

In order to be concrete, we will restrict ourselves in the following to the scattering from $N < \infty$ non-overlapping *disks* fixed in the 2-dimensional plane. The semiclassical approximation of the periodic itinerary

$$\mathrm{tr}\, \mathbf{A}^{s_1 s_2} \mathbf{A}^{s_2 s_3} \cdots \mathbf{A}^{s_{n-1} s_n} \mathbf{A}^{s_n s_1}$$

becomes a standard periodic orbit labeled by the symbol sequence $s_1 s_2 \cdots s_n$. Depending on the geometry, the individual legs $s_{i-1} \to s_i \to s_{i+1}$ result either from a standard specular reflection at disk s_i or from a ghost path passing straight through disk s_i. If furthermore creeping contributions are taken into account, the symbolic dynamics has to be generalized from single-letter symbols $\{s_i\}$ to triple-letter symbols $\{s_i, \sigma_i \times \ell_i\}$ with $\ell_i \geq 1$ integer

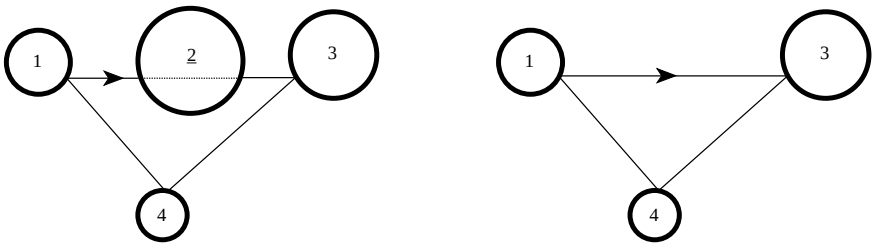

Figure 39.6: (a) The ghost itinerary $(1,\underline{2},3,4)$. (b) The parent itinerary $(1,3,4)$.

valued and $\sigma_i = 0, \pm 1$ [1] By definition, the value $\sigma_i = 0$ represents the non-creeping case, such that $\{s_i, 0 \times \ell_i\} = \{s_i, 0\} = \{s_i\}$ reduces to the old single-letter symbol. The magnitude of a nonzero ℓ_i corresponds to creeping sections of mode number $|\ell_i|$, whereas the sign $\sigma_i = \pm 1$ signals whether the creeping path turns around the disk s_i in the positive or negative sense. Additional full creeping turns around a disk s_i can be summed up as a geometrical series; therefore they do not lead to the introduction of a further symbol.

39.4.1 Ghost contributions

An itinerary with a semiclassical ghost section at, say, disk s_i can be shown to have the same weight as the corresponding itinerary without the s_i th symbol. Thus, semiclassically, they cancel each other in the tr $\ln(\mathbf{1} - \mathbf{A})$ expansion, where they are multiplied by the permutation factor n/r with the integer r counting the repeats. For example, let $(1,\underline{2},3,4)$ be a non-repeated periodic itinerary with a ghost section at disk 2 steming from the 4th-order trace tr A^4. By convention, an underlined disk index signals a ghost passage (as in figure 39.6a), with corresponding semiclassical ghost traversal matrices also underlined, $\underline{\mathbf{A}}^{i,\underline{i+1}}\underline{\mathbf{A}}^{\underline{i+1},i+2}$. Then its semiclassical, geometrical contribution to tr $\ln(\mathbf{1} - \mathbf{A})$ cancels exactly against the one of its "parent" itinerary $(1,3,4)$ (see figure 39.6b) resulting from the 3rd-order trace:

$$
\begin{aligned}
&-\frac{1}{4}\left(4\,\underline{\mathbf{A}}^{1,\underline{2}}\underline{\mathbf{A}}^{\underline{2},3}\mathbf{A}^{3,4}\mathbf{A}^{4,1}\right) - \frac{1}{3}\left(3\,\mathbf{A}^{1,3}\mathbf{A}^{3,4}\mathbf{A}^{4,1}\right) \\
&= \quad (+1-1)\,\mathbf{A}^{1,3}\mathbf{A}^{3,4}\mathbf{A}^{4,1} = 0\,.
\end{aligned}
$$

The prefactors $-1/3$ and $-1/4$ are due to the expansion of the logarithm, the factors 3 and 4 inside the brackets result from the cyclic permutation of the periodic itineraries, and the cancellation stems from the rule

⇓PRELIMINARY
38.5
page 723
⇑PRELIMINARY

$$
\cdots \underline{\mathbf{A}}^{i,\underline{i+1}}\underline{\mathbf{A}}^{\underline{i+1},i+2}\cdots = \cdots\left(-\mathbf{A}^{i,i+2}\right)\cdots\,. \tag{39.36}
$$

The reader might study more complicated examples and convince herself that the rule (39.36)(or (??) for the cases of adjacent ghost sections) is

⇓PRIVATE

IVATE

sufficient to cancel any primary or repeated periodic orbit with one or more ghost sections completely out of the expansion of $\mathrm{tr}\,\ln(\mathbf{1}-\mathbf{A})$ and therefore also out of the cumulant expansion in the semiclassical limit: Any periodic orbit of length m with $n(<m)$ ghost sections is cancelled by the sum of all 'parent' periodic orbits of length $m-i$ (with $1\le i\le n$ and i ghost sections removed) weighted by their cyclic permutation factor and by the prefactor resulting from the *trace-log* expansion. This is the way in which the nontrivial pruning for the N-disk billiards can be derived from the exact quantum mechanical expressions in the semiclassical limit. Note that there must exist at least one index i in any given *periodic* itinerary which corresponds to a non-ghost section, since otherwise the itinerary in the semiclassical limit could only be straight and therefore nonperiodic. Furthermore, the series in the ghost cancelation has to stop at the 2nd-order trace, $\mathrm{tr}\,\mathbf{A}^2$, as $\mathrm{tr}\,\mathbf{A}$ itself vanishes identically in the full domain which is considered here.

⇓PRELIMINARY

39.4.2 Semiclassical cycle weigth

AW: One of us has still to write these

regroup the terms in prime orbits (or refer to DasBuch section

write semiclassical cumulant expansion

truncated expansions

diffractive poles in 1-scatterer S-matrices

⇑PRELIMINARY

restore section3-disk system

39.5 Heisenberg uncertainty

Where is the boundary $ka\approx 2^{m-1}\bar{L}/a$ coming from?

This boundary follows from a combination of the uncertainty principle with ray optics and the non-vanishing value for the topological entropy of the 3-disk repeller. When the wave number k is fixed, quantum mechanics can only resolve the classical repelling set up to the critical topological order $n$given by (**??**). The quantum wave packet which explores the repelling set has to disentangle 2^n different sections of size $d\sim a/2^n$ on the "visible" part of the disk surface (which is of order a) between any two successive disk collisions. Successive collisions are separated spatially by the mean flight length $\bar{L}$, and the flux spreads with a factor $\bar{L}/a$. In other words, the uncertainty principle bounds the maximal sensible truncation in the cycle expansion order by the highest quantum resolution attainable for a given wavenumber k.

⇓PRIVATE
⇑PRIVATE

⇓PRELIMINARY

The upper limit n for which $c_m(k)$ with $m\le n$ approximates $Q_m(k)$ is increasing with increasing $\mathrm{Re}\,k$. For $n>m(\mathrm{Re}\,ka)$, defined in (**??**), the

[1] Actually, these are double-letter symbols as σ_i and l_i are only counted as a product.

cycle expansion terms and cumulant terms deviate so much from each other, that beyond this order the contributions of longer cycle expansions have nothing to do with quantum mechanics. The fact that $Z_{\rm GV}(k)|_n$ – even in its convergence regime – is a good approximation to quantum mechanics *only* up to a finite n is usually not noticed, as the terms in (**??**) are exponentially small on or close to the real axis and sum therefore to a tiny quantity. In other words, for $n > m(\mathrm{Re}\, ka)$ and close to the real k axis, the absolute error $|c_n(k) - Q_n(k)|$ is still small, the relative error $|c_n(k)/Q_n(k)|$ on the other hand is tremendous. With increasing negative $\mathrm{Im}\, k$, however, using the scaling rules (**??**) and (**??**), the deviations (**??**) are blown up, such that the relative errors $|c_n(k)/Q_n(k)|$ eventually become visible as absolute errors $|c_n(k) - Q_n(k)|$ (see e.g. the resonance calculation of ref. [M.1]). For $\mathrm{Im}\, k$ above the boundary of convergence these errors still sum up to a finite quantity which might, however, not be negligible any longer. Below the convergence line these errors sum up to infinity.

So, the value of Imk where — for a given n — the $Z_{\rm GV}(k)|_n$ sum deviates from $\det \mathbf{M}(k)|_n$ is governed by the real part of k and the scaling rules (**??**) and (**??**). It has nothing to do with the boundary of convergence of $Z_{GV}(k)$, as a good approximation is given by the *finite* sum of terms satisfying (**??**). Therefore, the truncated semiclassical expansion can describe the quantum mechanical resonance data even *below* the line of convergence of the infinite cycle expansion series, as we have already noted above.

On the other hand, the boundary line of the convergence regime of the semiclassical expansion is governed by $c_m(k)$, $m \to \infty$, terms which have nothing to do with the quantum analog $Q_m(k)$, i.e. solely by terms of type (**??**). The reason is that the convergence property of an infinite sum is governed by the *infinite* tail and not by the first few terms. Whether a semiclassical expansion converges or not is a separate issue from the question whether the quantum mechanical data are described well or not. The *convergence property* of a semiclassical zeta functions on the one hand and the *approximate description of quantum mechanics* by these zeta functions are therefore two different issues. It could happen that a zeta function is convergent, but not equivalent to quantum mechanics, as we have seen was the case with the extraneous resonances in the quasiclassical calculation. Or that it is not convergent in general, but its finite truncations nevertheless approximate well quantum mechanics, as is the case for the Gutzwiller-Voros zeta function

connect this to earlier text

$$Z_{\rm GV}(z;k) = \exp\left\{-\sum_p \sum_{r=1}^{\infty} \frac{1}{r} \frac{z^{rn_p}\, t_p^r}{1 - 1/\Lambda_p^r}\right\} = \prod_p \prod_{j=0}^{\infty} \left(1 - \frac{z^{n_p} t_p}{\Lambda_p^j}\right) , \quad (39.37)$$

where

$$t_p = e^{ikL_p - im_p\pi/2}/|\Lambda_p|^{\frac{1}{2}}$$

is the weight of the $p^{\rm th}$ prime cycle, n_p its topological length and z a

book-keeping variable for keeping track of the topological order in cycle expansions.

We conclude that the exponential rise of the number of cycles with increasing cycle expansion order n is the physical reason for the breakdown of the cycle expansion of the semiclassical zeta function(39.37) with respect to the exact quantum mechanical cumulant expansion.

Airy function
Debye approximation
Hankel function

⇑PRELIMINARY

Commentary

Remark 39.1 Sources. This chapter is based in its entirety on ref. [M.1]; the reader is referred to the full exposition for the proofs and discussion of details omitted here. sect. 39.3 is based on appendix E of ref. [M.1]. We follow Franz [38.19] in applying the Watson contour method [38.20] to (39.23). The Airy and Debye approximations to the Hankel functions are given in ref. [38.21], the Airy expansion of the 1-disk zeros can be found in ref. [38.22], see also ref. [**?**] for the expression of $\alpha_\ell(ka)$ to leading order. For details see refs. [38.19, 38.22, 38.23, M.1]. That the interior domains of the disks are excluded relatively to the free evolution without scattering obstacles was noted in refs. [38.24, 38.15].

change refs from Wirzba habilitation to Phys Reports throughout?

⇓PRIVATE

⇑PRIVATE

comment on Regge poles

The procedure for the semiclassical approximation of a general periodic itinerary (39.20) of length n can be found in ref. [M.1] for the case of the N-disk systems. The reader interested in the details of the semiclassical reduction is advised to consult this reference. For the case of grazing geometrical paths consult ref. [**?**]. In such cases we have coninciding saddles between the geometrical paths with $\pi/2$ angle reflection from the disk surface and paths with direct ghost tunneling through the disk.

⇓PRIVATE

⇑PRIVATE

The ghost orbits were introduced in refs. [38.12, 38.24].

merge with preceeding chapter?

Remark 39.2 Krein-Friedel-Lloyd formula. In the literature (see, e.g., refs. [38.14, 38.15] based on ref. [38.11] or ref. [38.1]) the transition from the quantum mechanics to the semiclassics of scattering problems has been performed via the semiclassical limit of the left hand sides of the Krein-Friedel-Lloyd sum for the (integrated) spectral density [M.5, M.6, 38.8, 38.9]. See also ref. [38.13] for a modern discussion of the Krein-Friedel-Lloyd formula and refs. [38.1, 38.17] for the connection of (38.17) to the the Wigner time delay.

find refref pinball

The order of the two limits in (38.18) and (38.17) is essential, see e.g. Balian and Bloch [38.11] who stress that smoothed level densities should be inserted into the Friedel sums.

The necessity of the $+i\epsilon$ in the semiclassical calculation can be understood by purely phenomenological considerations: Without the $i\epsilon$ term there is no reason why one should be able to neglect spurious periodic orbits which solely are there because of the introduction of the confining boundary. The subtraction of the second (empty) reference system helps just in the removal of those spurious periodic orbits which never encounter the scattering region. The ones that do would still survive the first limit $b \to \infty$, if they were not damped out by the $+i\epsilon$ term.

38.1
page 723

Remark 39.3 $\mathbf{T}$, $\mathbf{C}^s$, $\mathbf{D}^s$ and $\mathbf{A}^{ss'}$ matrices are trace-class In refs. [M.1] it has

find ref ,wh97

explicitly been shown that the $\mathbf{T}$-matrix as well as the $\mathbf{C}^s$, $\mathbf{D}^s$ and $\mathbf{A}^{ss'}$-matrices of the scattering problem from $N < \infty$ non-overlapping finite disks are all trace-class. The corresponding properties for the single-disk systems is particulary easy to prove.

⇓PRELIMINARY

??

page ??

Résumé

⇑PRELIMINARY

AW: still to add some more interesting exercises

create refsMultiscat